

Rabi oscillations in spasers during nonradiative plasmon excitation

E. S. Andrianov, A. A. Pukhov, A. V. Dorofeenko, and A. P. Vinogradov

Institute for Theoretical and Applied Electromagnetics of the Russian Academy of Sciences, 13 Izhorskaya, Moscow 125412, Russia

A. A. Lisiansky*

Department of Physics, Queens College of the City University of New York, Flushing, New York 11367, USA

(Received 20 October 2011; revised manuscript received 7 December 2011; published 5 January 2012)

In the approach to the stationary regime, a surface plasmon amplification by stimulated emission of radiation exhibits complicated and highly nonlinear dynamics with anharmonic oscillations [M. I. Stockman, *J. Opt.* **12**, 024004 (2010)]. We demonstrate that these oscillations are due to Rabi oscillations of the quantum dot in the field of the nanoparticle. We show that oscillations may or may not arise depending on the initial conditions.

DOI: [10.1103/PhysRevB.85.035405](https://doi.org/10.1103/PhysRevB.85.035405)

PACS number(s): 73.20.Mf, 42.50.Nn, 78.67.Pt, 81.05.Xj

I. INTRODUCTION

Recent discoveries in the area of nanoplasmonics, such as superlenses,¹ cloaking,^{1,2} hyperlenses,^{3–5} energy concentrators,⁶ and others, have raised high hopes for the future development of ultrafast and super small optoelectronic devices. The extremely small localization length of surface plasmons (SPs), which are the basic modes of nanoplasmonic devices, allows one to overcome the fundamental limitation of the optical wavelength.

At optical frequencies, the physical principle of plasmonic devices operation is based on the plasmonic resonance of a metallic nanoparticle (NP). The main disadvantage of these materials is their very high lossiness. One way to compensate for these losses is to include active (gain) inclusions.^{5,7–10} One of the most efficient and original types of active inclusion is the spaser (surface plasmon amplification by stimulated emission of radiation), which was first suggested in Ref. 11 and experimentally realized in Ref. 12. The spaser consists of a two-level quantum dot (QD) placed near a NP. The physical principle of the spaser's operation is similar to that of laser. The role of photons is played by SPs, which are localized at the NP.^{11,13–15} Confining SPs to the NP resembles a resonator. The spaser generates and amplifies the near field of the NP. SP amplification occurs because of nonradiative energy transfer from the QD to the NP. This process originates from the dipole-dipole (or any other near-field¹⁶) interaction between the QD and the plasmonic NP. This physical mechanism has high efficiency because the probability of exciting the SP excitation is $\sim(kr)^{-3}$ larger than the probability of radiative emission,¹⁷ where r is the distance between the centers of the NP and the QD and k is an optical wave number in vacuum. The generation of a large number of SPs leads to the induced emission of the QD into the plasmonic mode and to the development of generation of plasmons. Thus, the excitation of the plasmonic mode is provided by pumping through the excited QD. This process is inhibited by losses in the NP, which together with pumping results in undamped stationary oscillations of the spaser dipole moment. The key characteristic of spasers that determines their applicability in all-optical devices is the time required to establish the stationary regime of a nanoplasmonic element.

It may seem that spasers cannot be used as amplifiers due to the independence of the final amplitude of their

oscillations on the initial values of the near fields.¹⁸ However, recently Stockman¹⁵ has suggested the possibility of designing a spaser-based amplifier. Such an amplifier works during the transient regime, just after the population inversion has occurred but before the steady-state regime in the spaser is reached. The transient regime takes about 250 fs,¹⁵ during this time a spaser could amplify short optical pulses, making it an effective nanosize amplifier.

In the present paper, we study the dynamics of nonradiative plasmon excitations and investigate the emergence of SPs in a spaser and the conditions of establishing a steady-state regime. On the way to the stationary regime, a spaser exhibits complicated and highly nonlinear dynamics with anharmonic oscillations.¹⁵ We show that these oscillations are due to the Rabi oscillations of the QD in the field of the NP. The total time of the Rabi oscillations is smaller than the total transition regime time, which is determined by the relaxation of the QD polarization. We also show the Rabi oscillations arise only for large initial values of the SP amplitude.

II. THE EQUATION OF THE SPASER DYNAMICS

Following Refs. 11 and 19, let us consider the interaction between a metallic NP and a QD. For the simplest design of the spaser, it consists of a two-level QD of size r_{TLS} located at a distance r from the metal NP of size r in a solid dielectric or semiconductive medium. To describe the transition processes in such a spaser, one can use the model Hamiltonian of a metal NP interacting with a two-level QD in the form

$$\hat{H} = \hat{H}_{\text{SP}} + \hat{H}_{\text{TLS}} + \hat{V} + \hat{\Gamma}, \quad (1)$$

where

$$\hat{H}_{\text{SP}} = \hbar\omega_{\text{SP}}\hat{a}^\dagger\hat{a}, \quad (2a)$$

$$\hat{H}_{\text{TLS}} = \hbar\omega_{\text{TLS}}\hat{\sigma}^\dagger\hat{\sigma}. \quad (2b)$$

The Hamiltonian Eqs. (2a) and (2b) describe the NP and the two-level QD, respectively;^{11,20,21} the interaction between NP and QD is described by the operator $\hat{V} = -\hat{\mu}_{\text{TLS}} \cdot \hat{\mathbf{E}}_{\text{NP}}$, and the operator $\hat{\Gamma}$ describes all the effects of relaxation and pumping.²¹ Below we take into account dipole SPs only. In

Eq. (2a), $\hat{a}(t)$ is the Bose annihilation operator of the dipole SP so that the electric field of the NP has the form

$$\hat{\mathbf{E}}_{\text{NP}}(\mathbf{r}, t) = -A \nabla \varphi(\mathbf{r})(\hat{a}^\dagger + \hat{a}),$$

where $A = (4\pi\hbar s/\varepsilon_d s')^{1/2}$, $s' = d\text{Re}[s(\omega)]/d\omega|_{\omega=\omega_n}$, $s = [1 - \varepsilon_{\text{NP}}/\varepsilon_M]^{-1}$ is the Bergman spectral parameter and φ is the potential of the SP field, $\hat{\sigma} = |g\rangle\langle e|$ is the operator of the transition between the excited $|e\rangle$ and ground $|g\rangle$ states of the QD, $\hat{\mu}_{\text{TLS}} = \mu_{\text{TLS}}(\hat{\sigma}(t) + \hat{\sigma}^\dagger(t))$ is the dipole moment of the QD, and μ_{TLS} is its off-diagonal matrix element.

The SP wavelength, λ_{SP} , is much smaller than the optical wavelength in vacuum, λ ; therefore, the spatial derivatives in Maxwell equations are much larger than the temporal ones. Hence, the quasistatic approximation,²² in which the temporal derivatives are neglected, can be used for the description of the SP field. For example, at the SP resonant frequency, a small spherical NP of radius $r_{\text{NP}} \ll \lambda$ turns out to be a half-wavelength antenna (resonator), because the NP diameter is twice as small as the SP wavelength.²² Thus, one can find the frequency of the plasmonic resonance from the condition of existence of the nontrivial solution of the Laplace equation

$$\nabla \varepsilon(\mathbf{r}) \nabla \varphi(\mathbf{r}) = 0, \quad (3a)$$

in which $\varepsilon(\mathbf{r})$ equals ε_{NP} inside the NP and ε_M outside the NP in the dielectric matrix. The value ε_{NP} is considered as an eigenvalue of Eq. (3a). To separate the electromagnetic properties and the geometrical factor of the NP, it is convenient to represent the permittivity in the form¹² $\varepsilon(\mathbf{r}) = (\varepsilon_{\text{NP}} - \varepsilon_M)(\Theta(\mathbf{r}) - s)$, where the step function $\Theta(\mathbf{r})$ defines the geometry of the problem: it is equal to zero in the dielectric matrix and equal to unity inside the NP, whereas $s = [1 - \varepsilon_{\text{NP}}/\varepsilon_M]^{-1}$ only depends on constitutive properties of the system. By using such notation the Laplace equation may be written in the form^{13,15}

$$\nabla \Theta(\mathbf{r}) \nabla \varphi(\mathbf{r}) = s \nabla^2 \varphi(\mathbf{r}), \quad (3b)$$

which allows one to find the eigenvalues s_n and eigenfunctions $\varphi_n(\mathbf{r})$, $n = 1, 2, \dots$. In the particular case of a spherical NP, the n -th plasmonic multipole has the resonance at $\varepsilon_{\text{NP}} = -\varepsilon_M(n+1)/n$ and $s_n = n/(2n+1)$.^{17,20,22}

By taking into account the permittivity dispersion, $\varepsilon_{\text{NP}}(\omega)$, the eigenfrequency Ω_n is determined from the condition $s(\Omega_n) = [1 - \varepsilon_{\text{NP}}(\Omega_n)/\varepsilon_M]^{-1} = s_n$. In the general case, due to the Joule losses in the metallic NP, the eigenfrequency has an imaginary part: $\Omega_n = \omega_n - i\gamma_n$. In addition, there are radiation losses of the NP due to the oscillation of a SP multipole. Let us estimate the values of both types of losses. In the case of the dipole SP, the part of losses associated with the emission of photons to free space can be estimated as

$$P_{\text{rad}} = \frac{2}{3c^3} \omega^4 \mu_{\text{NP}}^2 = \frac{2}{27c^3} \omega^4 |E_{\text{NP}}|^2 r_{\text{NP}}^6 (\varepsilon - 1)^2, \quad (4)$$

where we take into account the relationship between the dipole moment with a homogeneous field inside the spherical NP and

the external field: $\mu_{\text{NP}} = Er_{\text{NP}}^3(\varepsilon - 1)/3$. At the same time, the power absorbed due to Joule losses is

$$\begin{aligned} P_{\text{Joule}} &= \frac{\omega}{8\pi} \int \varepsilon'' |E_{\text{NP}}|^2 dV \approx \frac{\omega}{8\pi} \varepsilon'' |E|_{\text{NP}}^2 \frac{4}{3} \pi r^3 \\ &= \frac{1}{6} r^3 \omega \varepsilon'' |E_{\text{NP}}|^2. \end{aligned} \quad (5)$$

The ratio of these quantities is

$$\frac{P_{\text{rad}}}{P_{\text{Joule}}} = \frac{4(\varepsilon - 1)^2}{9\varepsilon''} (k_0 r)^3. \quad (6)$$

For the NP of size 10 nm this ratio is ~ 0.06 . Thus, for small NPs Joule losses far exceed the loss due to radiation. This means that a spaser mainly generates the near field. However, for particles of size 20 nm, $P_{\text{rad}}/P_{\text{Joule}} \sim 0.5$ and the emission will be detected in far fields.

In this paper, we assume that the size of the NP is small and disregard the radiative losses. The imaginary part of the resonance frequency may be estimated as $\gamma_a = \omega \varepsilon'' [\partial(\omega \varepsilon')/\partial \omega]^{-1}$. For example, for a silver NP in the optical range, $\gamma_a/\omega \sim 0.05$. We only consider the excitation of the main (dipole) mode with the frequency ω_{SP} . The dipole moment of a spherical NP induced by the quasistatic field \mathbf{E}_{TLS} of a QD with a dipole moment μ_{TLS} is equal to²³

$$\begin{aligned} \mu_{\text{SP}} &= r_{\text{NP}}^3 \left(\frac{\varepsilon_{\text{NP}} - \varepsilon_M}{\varepsilon_{\text{NP}} + 2\varepsilon_M} \right) \mathbf{E}_{\text{TLS}} = \left(\frac{r_{\text{NP}}}{r} \right)^3 \left(\frac{\varepsilon_{\text{NP}} - \varepsilon_M}{\varepsilon_{\text{NP}} + 2\varepsilon_M} \right) \\ &\times \left[\frac{3(\mu_{\text{TLS}} \cdot \mathbf{r}) \mathbf{r}}{r^2} - \mu_{\text{TLS}} \right]. \end{aligned} \quad (7)$$

Using the value of the permittivity for the silver NP surrounded by silicon oxide,²⁴ we estimate the dipole moment of the NP, $\mu_{\text{SP}}(\omega)$. The dipole moment of a typical QD of size $r_{\text{TLS}} \sim 10\text{nm}$ equals $\mu_{\text{TLS}} \approx 20D$.²⁵ Assuming $r_{\text{NP}} \sim r \sim 10\text{nm}$, we obtain $\mu_{\text{NP}} \sim 200D$ close to the plasmonic resonance. In turn, this allows one to estimate the energy of the static dipole-dipole interaction between the NP and the QD, $V = \hbar \Omega_R \sim \mu_{\text{NP}} \mu_{\text{TLS}} / r^3$. This gives $\Omega_R \approx 5 \cdot 10^{12} \text{s}^{-1} \ll \omega_{\text{SP}}$.

If the QD transition frequency is close to the frequency of SPs, $\omega_{\text{SP}} \approx \omega_{\text{TLS}}$, one can assume that the time dependence of operators $\hat{a}(t)$ and $\hat{\sigma}(t)$ has the form $\hat{a}(t) \equiv \hat{a}(t)e^{-i\omega t}$ and $\hat{\sigma}(t) \equiv \hat{\sigma}(t)e^{-i\omega t}$, where $\hat{a}(t)$ and $\hat{\sigma}(t)$ are the slowly varying amplitudes. Neglecting the fast oscillating terms $\sim e^{\pm 2i\omega t}$ (the rotating-wave approximation), the interaction operator can be written in the Jaynes-Cummings form²⁶

$$\hat{V} = \hbar \Omega_R (\hat{a}^\dagger \hat{\sigma} + \hat{\sigma}^\dagger \hat{a}), \quad (8)$$

where Ω_R is the Rabi frequency. The commutation relations for operators $\hat{a}(t)$ and $\hat{\sigma}(t)$ are standard: $[\hat{a}, \hat{a}^\dagger] = \hat{1}$ and $[\hat{\sigma}^\dagger, \hat{\sigma}] = \hat{D}$, where $\hat{D}(t) = \hat{n}_e(t) - \hat{n}_g(t)$ is the population inversion operator, $\hat{n}_e = |e\rangle\langle e|$ and $\hat{n}_g = |g\rangle\langle g|$ are operators of the populations of the upper and lower levels of the QD, $\hat{n}_e + \hat{n}_g = 1$. Using Hamiltonian (1), we obtain the Heisenberg equations of motion for operators $\hat{a}(t)$, $\hat{\sigma}(t)$,

and $\hat{D}(t)$ ^{13,19}

$$\dot{\hat{D}} = 2i\Omega_R(\hat{a}^\dagger\hat{\sigma} - \hat{\sigma}^\dagger\hat{a}) - \frac{\hat{D} - \hat{D}_0}{\tau_D}, \quad (9)$$

$$\dot{\hat{\sigma}} = (i\delta - \tau_\sigma^{-1})\hat{\sigma} + i\Omega_R\hat{a}\hat{D}, \quad (10)$$

$$\dot{\hat{a}} = (i\Delta - \tau_a^{-1})\hat{a} - i\Omega_R\hat{\sigma}, \quad (11)$$

where $\delta = \omega - \omega_{\text{TLS}}$ and $\Delta = \omega - \omega_{\text{SP}}$ are frequency detunings. Because the time exponents in $\hat{n}_e = |e\rangle\langle e|$ and $\hat{n}_g = |g\rangle\langle g|$ are cancelled, the operator of the population inversion $\hat{D}(t)$ is slow. The time-constants τ_D , τ_σ , and τ_a are introduced in order to take into account the relaxation processes and the pumping term. The operator \hat{D}_0 describes pumping. The population inversion operator \hat{D}_0 plays the role of operator \hat{D} in the regime of absence of generation. In other words, without generation $\{\hat{D} = \hat{D}_0, \hat{a} = \hat{\sigma} = \hat{0}\}$ is a stable fixed point of Eqs. (9)–(11). In the case in which generation exists, this fixed point becomes unstable (see below for details).^{21,26}

Below we neglect the quantum fluctuations and correlations and consider $\hat{D}(t)$, $\hat{\sigma}(t)$ and $\hat{a}(t)$ as complex quantities (*c*-numbers), substituting the Hermitian conjugation by the complex conjugation.^{10,15,19,23} The $D(t)$ is a real valued quantity because the corresponding operator is Hermitian. The values of $\sigma(t)$ and $a(t)$ represent the complex amplitudes of the oscillations of the dipole moments of the QD and the NP, respectively.

III. STATIONARY REGIME OF SPASER LASING

The system of Eqs. (9)–(11) has a nontrivial stationary solution. Assuming that temporal derivatives equal zero, we reduce these equations to

$$2i\Omega_R(a^*\sigma - \sigma^*a) - \frac{D - D_0}{\tau_D} = 0, \quad (12)$$

$$(i\delta - \tau_\sigma^{-1})\sigma + i\Omega_R a D = 0, \quad (13)$$

$$(i\Delta - \tau_a^{-1})a - i\Omega_R\sigma = 0. \quad (14)$$

Eliminating σ from Eqs. (13) and (14), we obtain

$$\left[\frac{(i\delta - \tau_\sigma^{-1})(i\Delta - \tau_a^{-1})}{i\Omega_R} + i\Omega_R D \right] a = 0. \quad (15)$$

Besides the trivial solution, $a = 0$, $\sigma = 0$, and $D = D_0$, there is a nontrivial solution corresponding to lasing. The complex expression in square brackets gives two real relations

$$\tau_\sigma\delta = -\tau_a\Delta, \quad (16)$$

$$D = D_{\text{th}} = \frac{1 + \Delta^2\tau_a^2}{\Omega_R^2\tau_a\tau_\sigma}. \quad (17)$$

The lasing frequency is given by Eq. (16):

$$\omega = \frac{\omega_{\text{SP}}\tau_a + \omega_{\text{TLS}}\tau_\sigma}{\tau_a + \tau_\sigma}. \quad (18)$$

The frequency defined by Eq. (18) is always located between frequencies of NP and QD.^{11,19} From Eqs. (8)–(10)

and (13), we find the stationary amplitude of NP and QD dipole moments

$$a = \frac{e^{i\psi}}{2} \sqrt{\frac{(D_0 - D_{\text{th}})\tau_a}{\tau_D}}, \quad (19)$$

$$\sigma = a \frac{\Delta + i\tau_a^{-1}}{\Omega_R}, \quad (20)$$

where ψ is an arbitrary constant phase. Because $D \leq D_0 \leq 1$, the nontrivial stationary solution has physical meaning only if $D_{\text{th}} < 1$ or

$$\Omega_R^2\tau_a\tau_\sigma > 1 + \Delta^2\tau_a^2. \quad (21)$$

Equation (21) is a necessary condition for spasing: if this condition is satisfied and $D_0 > D_{\text{th}}$, the nontrivial stationary solutions given by Eqs. (17), (19), and (20) exist. This means that nonzero dipole moments of the NP and the QD are excited, i.e., the spaser generates plasmons. For the parameters used in our consideration, the spaser threshold is $D_{\text{th}} \sim 0.1$. This value is small enough to be achieved experimentally.¹²

IV. TRANSIENT REGIME

The system of Eqs. (9)–(11) is nonlinear; therefore, the establishing of the steady-state regime can be investigated only numerically. Our computer simulation shows that the system evolution strongly depends on initial conditions and on the relations between relaxation times τ_a , τ_σ , and τ_D (see also Ref. 15). As one can see from Fig. 1, this evolution can be either monotonic or have an oscillatory character.

The dynamics of the transition regime is characterized by the energy exchange between the SP of the NP and the QD excitation. The phase difference $\Delta\varphi = \arg[\sigma(t)/a(t)]$

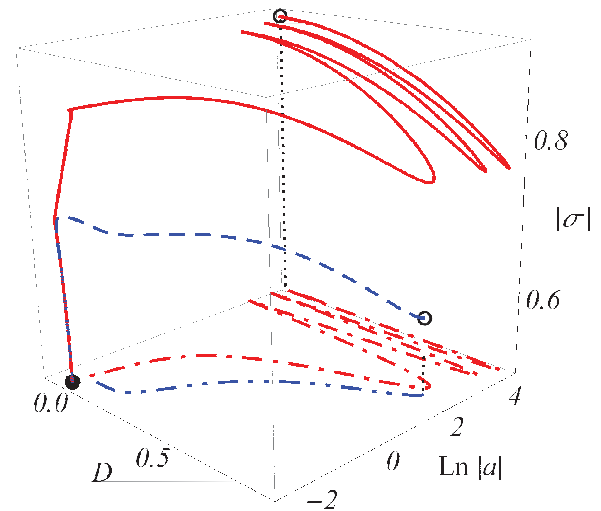


FIG. 1. (Color online) The evolution of the spaser. The open circles mark the beginning of the transient regime, then the system moves along either the solid line ($a(0) = 40 + 25i, \sigma(0) = 0.9$, and $D(0) = 0.05$) or the dashed line ($a(0) = 5, \sigma(0) = 0.65$, and $D(0) = 0.9$) until it reaches the stationary state marked by the solid circle. Dash-dotted and dash-double dotted lines are projections of the trajectories on the plane $|\sigma| = 0.5$. The curves shown were calculated for the time-constants $\tau_a = 10^{-14}$ s, $\tau_\sigma = 10^{-11}$ s, $\tau_D = 10^{-13}$ s, and $\Omega_R = 10^{13}$ s⁻¹.

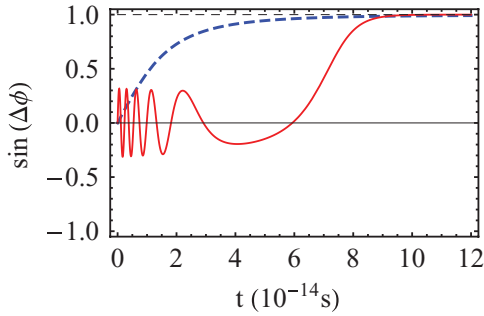


FIG. 2. (Color online) The dependence of the phase mismatch on time. The initial conditions corresponding to solid line and dashed lines are $a(0) = 50i$, $\sigma(0) = 0.25$, and $D(0) = 0.6$, and $a(0) = 0.1$, $\sigma(0) = 0.5$, and $D(0) = 0.7$, respectively. Values of the time constants and the Rabi frequency are the same as in Fig. 1.

between the QD polarization and the SP is responsible for the energy flux.²⁷ In particular, the sign of $\sin \Delta\varphi$ determines the direction of the flux. Thus, oscillations of $\sin \Delta\varphi$ indicate the change in the direction of the energy flux.

The time dependence of $\Delta\varphi$ is sensitive to the initial values of a , σ , and D . Note, that the latter quantity according to their physical meanings should be chosen within the intervals $-1 \leq D(0) \leq 1$ because $D(0) = n_e(0) - n_g(0)$ and $0 \leq n_e(0) \leq 1$, $n_g(0) = 1 - n_e(0)$. For small initial values of the SP amplitude, $a(0) \ll 1$, the system parameters do not oscillate. The transition time is determined by the relaxation time τ_σ . The value of $\sin \Delta\varphi(t)$ increases monotonically from the initial value, which is equal to zero, to the steady-state value that corresponds to the energy flux directed from the QD to the NP (the dashed line in Fig. 1 and the solid line in Fig. 2).

For large initial values of the SP amplitude, $a(0) \gg 1$, the variables a , σ , and D exhibit oscillations as shown in Figs. 1 and 3. In this case, the transient regime splits into two stages. At the first stage, which lasts $\sim \tau_a \ln |a(0)|$, there are the Rabi oscillations with the characteristic period $\sim \pi / \Omega_R |a(0)|$. The total number of oscillations N depends on the initial plasmon amplitude, $N \sim \tau_a \Omega_R |a(0)| \ln |a(0)|$. During the second stage, the QD polarization gradually reaches the stationary value without oscillations (see Fig. 3).

At the first stage, $\sin \Delta\varphi(t)$ oscillates (the solid line in Fig. 2). This indicates that the energy flux changes its direction.

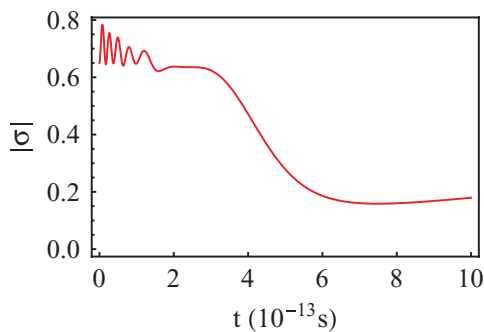


FIG. 3. (Color online) The dependence of the QD polarization on time calculated for the initial conditions $a(0) = 10$, $\sigma(0) = 0.65$, and $D(0) = 0.2$. All other parameters have the same values as in previous figures.

Thus, the energy can flow not only from the QD to the NP but also from the NP to the QD.

V. RABI OSCILLATIONS OF NONRADIATIVE SPASER EXCITATIONS

To estimate the frequency of the oscillations observed in the computer simulation,¹⁵ for simplicity, we consider the case of the exact resonance $\delta = \Delta = 0$. Then the system of Eqs. (9)–(11) has the form

$$\dot{a} = -i\Omega_R \sigma, \quad (22)$$

$$\dot{\sigma} = i\Omega_R a D, \quad (23)$$

$$\dot{D} = 2i\Omega_R (a^* \sigma - \sigma^* a). \quad (24)$$

During the first stage, when all dynamic variables of the spaser are far from their stationary values, the time derivatives are much greater than respective terms proportional to the inverse relaxation times; therefore, we can omit the terms responsible for the relaxation and pumping. The substitution of Eq. (22) and its conjugate into Eq. (24) gives

$$\dot{D} = -2(a^* \dot{a} + \dot{a}^* a) = -2 \frac{d|a|^2}{dt}. \quad (25)$$

This leads to the following integral of motion

$$D + 2|a|^2 = C_1, \quad (26)$$

where $C_1 = D(0) + 2|a(0)|^2$. Representing a in the form $a = |a|e^{i\varphi}$ and differentiating Eq. (22) with respect to time, we obtain

$$\left[\frac{d^2|a|}{dt^2} - |a| \left(\frac{d\varphi}{dt} \right)^2 + i \left(2 \frac{d\varphi}{dt} \frac{d|a|}{dt} + |a| \frac{d^2\varphi}{dt^2} \right) \right] e^{i\varphi} = i\Omega_R \frac{d\sigma}{dt}. \quad (27)$$

Using Eqs. (23), (25), and (27), we can split Eq. (27) into two equations

$$2 \frac{d\varphi}{dt} \left| \frac{da}{dt} \right| + |a| \frac{d^2\varphi}{dt^2} = 0, \quad (28)$$

$$\frac{d^2|a|}{dt^2} - |a| \left(\frac{d\varphi}{dt} \right)^2 = \Omega_R^2 |a| (C_1 - 2|a|^2). \quad (29)$$

From Eq. (28) it is clear that

$$|a| \left(2 \frac{d\varphi}{dt} \left| \frac{da}{dt} \right| + |a| \frac{d^2\varphi}{dt^2} \right) = \frac{d}{dt} \left(|a|^2 \frac{d\varphi}{dt} \right) = 0. \quad (30)$$

As the result, we obtain the second integral of motion $|a|^2 (d\varphi/dt) = C_2$. Let us suppose that $C_2 = 0$, which can always be achieved by the appropriate choice of initial conditions. Then $d\varphi/dt = 0$, and from Eq. (29) we obtain

$$\frac{d^2|a|}{dt^2} = \Omega_R^2 |a| (C_1 - 2|a|^2). \quad (31)$$

Equation (31) represents Newton's equation for a unit mass particle with the coordinate $|a|$ moving in the potential $U(|a|) = (\Omega_R^2 |a|^4 - C_1 \Omega_R^2 |a|^2) / 2$. The stable equilibrium position of such a particle is $|a|_{\text{eq}} = \sqrt{C_1/2} = \sqrt{|a(0)|^2 + D(0)/2} \approx |a(0)|$. Thus, the particle

exhibits oscillations about this equilibrium position with the frequency

$$\Omega = 2|a(0)|\Omega_R \quad (32)$$

and the small amplitude $D(0)/(2|a(0)|)$. Equation (32) coincides with the known expression for the frequency of Rabi oscillations, which occur for the interaction of a two-level QD with the classical harmonic field of the amplitude $a(0)$ or the quantized field with the number of quanta $\hat{a}^+(0)\hat{a}(0) = n = |a(0)|^2$.²⁶ In addition, Eq. (32) is in full agreement with the simulation results. Therefore, we can conclude that the phase oscillations observed in the numerical simulation are Rabi oscillations of QD populations in the NP near field.

VI. DISCUSSION OF RESULTS

Our numerical simulation shows that in the stationary regime, similar to the case of the interaction of two classical dipoles,²⁷ the excitation of the NP by the QD near field is possible only if there is the phase difference, $\Delta\varphi$, between the dipole moments of the QD and the NP. When $\sin \Delta\varphi$ is positive, the energy provided by the pump in the QD is transmitted to the NP and then is dissipated in the form of loss. During the transition regime the direction of the energy flow may change several times.

The spaser transition to the stationary auto-oscillations is determined by three characteristic times: the relaxation time of the SP amplitude, τ_a , the relaxation time of the QD polarization, τ_σ , and the relaxation time of the population inversion, τ_D . τ_a stems from Joule losses in metal NP. Because of extremely high losses in metals, this time is the shortest. Its experimentally measured value is 10^{-14} – 10^{-13} s²⁸ that coincides with estimates obtained from classical electrodynamics.⁹ The typical values of τ_σ and τ_D known from experiments are 10^{-11} s and 10^{-13} s, respectively.^{29–31} Thus, for metal NPs and semiconductor nanocrystal QDs, typical relations for times τ_a ,

τ_D , and τ_σ are $\tau_a < \tau_D \ll \tau_\sigma$. The total transition is determined by the largest time τ_σ .

The character of the transient process is greatly affected by the initial value of the SP amplitude $a(0)$. For the “cold start” of the spaser, when the initial value of SPs is due to the spontaneous emission of a QD, $a(0)$ is small. Then the electric field of the SP is of the order of the field of the dipole moment of the QD, and the Rabi oscillations do not arise and the energy flows monotonically from the QD to the NP. A large value of $a(0)$ can be obtained by exciting SPs with a nanosecond pulse of an optical parametric oscillator.¹² In this case, the transition process is more complicated. It can be divided into two stages. During the first stage, when the QD is in the high field of the SP, the Rabi oscillations with the characteristic period $\tau_R = \Omega_R^{-1}$ arise (see Fig. 3), and the energy flux oscillates between the QD and the SP. During the time $\sim \tau_a \ln|a(0)|$, these oscillations die out because of dissipation. During the second stage, the spaser exhibits a behavior observed at small $a(0)$, the transient regime continues until the spaser starts stationary auto-oscillations. The total time of the transient regime is $\sim \tau_\sigma$. For $\tau_a < \tau_D \ll \tau_\sigma$, the picture depends weakly on the value of τ_D .

During the period in which stationary spaser oscillations are established, the spaser can be used as an amplifier or a switch. The total duration of the transition regime is determined by the relaxation of the QD polarization, τ_σ . Thus, one should use QDs with slow relaxation in designing a nanoamplifier, while using QDs with fast relaxation is preferable for ultrafast switching.

ACKNOWLEDGMENTS

The authors are indebted to B. Luk'yanchuk for useful discussions. This work was supported by RFBR Grants Nos. 10-02-91750, 10-02-92115, and 11-02-92475 and by a PSC-CUNY grant.

*alexander.lisyansky@qc.cuny.edu

¹J. B. Pendry, *Phys. Rev. Lett.* **85**, 3966 (2000).

²U. Leonhardt, *IEEE J. Sel. Top. Quantum Electron.* **9**, 102 (2003).

³P. A. Belov, C. R. Simovski, and P. Ikonen, *Phys. Rev. B* **71**, 193105 (2005).

⁴Z. Liu, H. Lee, Y. Xiong, C. Sun, and X. Zhang, *Science* **315**, 1686 (2007).

⁵S. A. Ramakrishna and J. B. Pendry, *Phys. Rev. B* **67**, 201101 (2003).

⁶J. Yang, M. Huang, C. Yang, Z. Xiao, and J. Peng, *Opt. Express* **17**, 19656 (2009).

⁷A. K. Sarychev and G. Tartakovsky, *Proc. SPIE* **6320**, 6300A (2006).

⁸A. K. Sarychev, A. A. Pukhov, and G. Tartakovsky, *PIERS Online* **3**, 1264 (2007).

⁹A. K. Sarychev and G. Tartakovsky, *Phys. Rev. B* **75**, 085436 (2007).

¹⁰A. N. Lagarkov, A. K. Sarychev, V. N. Kissel, and G. Tartakovsky, *Phys. Usp.* **52**, 959 (2009).

¹¹D. J. Bergman and M. I. Stockman, *Phys. Rev. Lett.* **90**, 027402 (2003).

¹²M. A. Noginov, G. Zhu, A. M. Belgrave, R. Bakker, V. M. Shalaev, E. E. Narimanov, S. Stout, and E. Herz, *Nature* **460**, 1110 (2009).

¹³K. Li, X. Li, M. I. Stockman, and D. J. Bergman, *Phys. Rev. B* **71**, 115409 (2005).

¹⁴M. I. Stockman, *Nat. Photonics* **2**, 327 (2008).

¹⁵M. I. Stockman, *J. Opt.* **12**, 024004 (2010).

¹⁶I. R. Gabitov, B. Kennedy, and A. I. Maimistov, *IEEE J. Sel. Top. Quantum Electron.* **16**, 401 (2010).

¹⁷V. V. Klimov, *Phys. Usp.* **51**, 839 (2008).

¹⁸M. Premaratne and G. P. Agrawal, *Light Propagation in Gain Medium* (Cambridge University Press, New York, 2011).

¹⁹I. E. Protsenko, A. V. Uskov, O. A. Zaimidoroga, V. N. Samoilov, and E. P. O'Reilly, *Phys. Rev. A* **71**, 063812 (2005).

²⁰L. Novotny and B. Hecht, *Principles of Nano-Optics* (Cambridge University Press, New York, 2006).

²¹R. H. Pantell and H. E. Puthoff, *Fundamentals of Quantum Electronics* (Wiley, New York, 1969).

²²V. S. Zuev and G. Y. Zueva, *Opt. Spectrosc.* **107**, 614 (2009).

²³A. S. Rosenthal and T. Ghannam, *Phys. Rev. A* **79**, 043824 (2009).

- ²⁴E. D. Palik, *Handbook of Optical Constants of Solids* (Academic Press, New York, 1985).
- ²⁵A. Muller, Q. Q. Wang, P. Bianucci, C. K. Shih, and Q. K. Xue, *Appl. Phys. Lett.* **84**, 981 (2004).
- ²⁶M. O. Scully and M. S. Zubairy, *Quantum Optics* (Cambridge University Press, Cambridge, 1997).
- ²⁷A. A. Kolokolov and G. V. Skrotskii, *Sov. Phys. Usp.* **35**, 1089 (1992).
- ²⁸F. Stietz, J. Bosbach, T. Wenzel, T. Vartanyan, A. Goldmann, and F. Träger, *Phys. Rev. Lett.* **84**, 5644 (2000).
- ²⁹T. S. Sosnowski, T. B. Norris, H. Jiang, J. Singh, K. Kamath, and P. Bhattacharya, *Phys. Rev. B* **57**, R9423 (1998).
- ³⁰M. Bayer and A. Forchel, *Phys. Rev. B* **65**, 041308 (2002).
- ³¹J. M. Harbold, H. Du, T. D. Krauss, K.-S. Cho, C. B. Murray, and F. W. Wise, *Phys. Rev. B* **72**, 195312 (2005).